

Observation of keratin particles showing fast bidirectional movement colocalized with microtubules

Mirjana Livovic^{1,2}, Mette M. Mogensen³, Alan R. Prescott¹ and E. Birgitte Lane^{1,*}

¹Division of Cell and Developmental Biology, School of Life Sciences, University of Dundee, Dundee DD1 5EH, UK

²Medical Centre for Molecular Biology, Medical Faculty, University of Ljubljana, SI-1000, Slovenia

³School of Biological Sciences, University of East Anglia, Norwich NR4 7TJ, UK

*Author for correspondence (e-mail: e.b.lane@dundee.ac.uk)

Accepted 9 January 2003

Journal of Cell Science 116, 1417-1427 © 2003 The Company of Biologists Ltd

doi:10.1242/jcs.00363

Summary

Keratin intermediate filament networks were observed in living cultured epithelial cells using the incorporation of fluorescently tagged keratin from a transfected enhanced green fluorescent protein (EGFP) construct. In steady-state conditions EGFP-keratin exists not only as readily detectable intermediate filaments, but also as small particles, of which there are two types: a less mobile population (slow or static S particles) and a highly dynamic one (fast or F particles). The dynamic F particles move around the cell very fast and in a non-random way. Their movement is composed of a series of steps, giving an overall characteristic zig-zag trajectory. The keratin particles are found all over the cell and their movement is aligned with microtubules; treatment of cells with nocodazole has an inhibitory effect on keratin particle movement, suggesting

the involvement of microtubule motor proteins. Double-transfection experiments to visualize tubulin and keratin together suggest that the movement of keratin particles can be bidirectional, as particles are seen moving both towards and away from the centrosome area. Using field emission scanning and transmission electron microscopy combined with immunogold labelling, we also detected particulate keratin structures in untransfected epithelial cells, suggesting that keratin particles may be a natural component of keratin filament dynamics in living cells.

Movies available online

Key words: Intermediate filaments, Keratins, Microtubules, Epidermolysis bullosa simplex, Microscopy

Introduction

Over the past quarter of a century, analysis of the substructure of cells has been built substantially on the use of specific antibodies. However, immunofluorescence labelling of cell components requires the cell to be chemically or physically damaged so that cell structures can be exposed to the antibodies; it also causes the unavoidable generation of artifacts. The use of green fluorescent protein (GFP) hybrid constructs now enables live-cell imaging of specific components, offering a new perspective of cell structures and processes.

Keratins are members of the intermediate filament family of proteins that form an intricate network running through the cytoplasm of eukaryotic cells, and, together with microfilaments and microtubules, they make up the cytoskeleton. They are characterized by strikingly tissue-specific expression patterns from early embryogenesis onwards, suggesting that these major structural proteins are important in defining tissue structure and potential function.

Understanding the assembly and maintenance of intermediate filament networks *in vivo* is still a challenge to cell biology. Intermediate filament assembly *in vitro* is not energy dependent and does not require any associated proteins. A consensus hypothetical assembly sequence is now emerging from many laboratories, on the basis of *in vitro* assembly studies (Steinert et al., 1993a; Steinert et al., 1993b; Herrmann

et al., 1999), as follows: monomeric subunits first dimerize in parallel and in register; dimers then assemble into one of the several possible antiparallel (mostly staggered) alignments, giving rise to tetramers, which are the major soluble subunits identifiable *in vivo* (Quinlan et al., 1984; Soellner et al., 1985; Chou et al., 1993). *In vitro*, tetramers associate laterally into unit length filaments (ULFs) of around 60 nm long and 16 nm wide, which then anneal longitudinally to form loosely packed immature filaments. Further filament maturation then occurs without change in mass per length as filaments become more compact, reducing their diameter to about 10 nm (Herrmann and Aebi, 1998; Herrmann et al., 1999). All of these stages have been deduced from tracking *in vitro* polymerization, but so far they have not all been identified in living cells.

The identification of mutations in keratin genes is helping to define the structural role of intermediate filaments as an increasing number of human diseases are being linked to mutations in keratins and other intermediate filaments – see, for example, The Human Intermediate Filament Database (<http://www.interfil.org>). Pathogenic mutations appear to compromise the filament network assembly characteristics and may therefore shed some light on the function of specific subdomains. In particular, mutations in keratins, the epithelial intermediate filament structural proteins, have been shown to cause a range of genodermatoses (for reviews, see Irvine and McLean, 1999; Coulombe and Omary, 2002). All intermediate

filament proteins share a similar structure consisting of a central α -helical rod domain and N- (head) and C-terminal (tail) domains, and most pathogenic keratin mutations lie in the conserved peptide motifs located at either end of the rod domain. This concurs with *in vitro* experiments showing that these helix boundary sequences are important for efficient polymerization and that mutations here will often interfere with dimer formation or impair dimer stability (Herrmann et al., 2000; Wu et al., 2000; Wang et al., 2000a; Mehrani et al., 2001). In addition to the rod end mutation 'hot-spots', mutation cluster sites also occur in other places: in the head domain adjacent to the amino terminal end of the rod domain, in the non-helical linker domain in the middle of the rod domain, and slightly further inside the rod ends. These secondary cluster sites, however, are typically associated with milder disease phenotypes than those associated with the hot-spots of the helix boundary motif sites. The differences in disease severity associated with different mutation sites on the keratin proteins is most apparent in the case of keratin (K5) and K14 (Lane, 1994), although there are some exceptions to this (Liovic et al., 2001). K5 and K14 are the major intermediate filament components of epithelial basal cells throughout the body and are important structural components of the epidermis. Mutations in K5 and K14 cause epidermal basal cell lysis after mild trauma to the skin (epidermolysis bullosa simplex, or EBS). Severe cases of EBS, the so-called Dowling–Meara form of the disease, show clusters of blisters at any site in the body, and are associated with mutations in the helix boundary peptides of K5 or K14. Mutations outside the helix boundary peptides in K5 or K14 are generally associated with milder (Weber-Cockayne) EBS forms, in which blistering is limited to hands and feet. The Dowling–Meara mutations, but not Weber-Cockayne mutations, cause substantial abnormalities in keratin assembly *in vivo*, and electron-dense keratin aggregates are visible by electron microscopy in some Dowling–Meara epidermal cells (Anton-Lamprecht and Schnyder, 1982; Haneke and Anton-Lamprecht, 1982). These aggregates are diagnostic of this form of EBS and were the structures in which keratin abnormalities were first shown (Ishida-Yamamoto et al., 1991). The nature and origin of these aggregates in relation to keratin assembly processes is unclear, as is their role in the development of EBS lesions. There is therefore a need for closer analysis of keratin assembly and disassembly dynamics in normal and mutant cells so that new routes to intervention therapy for these skin fragility diseases can be identified.

The overall emerging picture of intermediate filament function has thus been one of stable filament systems, which provide physical resilience to cells. All the more striking, therefore, are several recent studies on live cells using GFP-tagged intermediate filament proteins vimentin (Pralhad et al., 1998; Yoon et al., 1998; Ho et al., 1998) or keratins K8, K18 or K13 (Windoffer and Leube, 1999; Strnad et al., 2001; Yoon et al., 2001; Windoffer and Leube, 2001), which have revealed these filament networks to be flexible and dynamic structures. The first papers using this type of analysis of intermediate filaments showed that filament movement appears to be at least partly dependent on an intact microtubule filament system (Pralhad et al., 1998; Yoon et al., 1998; Windoffer and Leube, 1999). Flux in the system was detectable as continuous lateral subunit exchange along the filament length, taking place

between the filaments and a 'soluble' protein pool (Yoon et al., 1998; Yoon et al., 2001). Significant differences were observed between vimentin and keratin intermediate filaments. For example, the subunit exchange rate calculated from fluorescence recovery after photobleaching (FRAP) experiments is almost 20 times faster for vimentin than for keratin intermediate filaments (Yoon et al., 2001). Some studies have also described large fragments of filaments (squiggles), which may constitute part of the assembly process (Pralhad et al., 1998; Yoon et al., 2001).

In this paper we present observations from a live-cell-imaging study of epithelial cells transfected with a fluorescently tagged keratin construct [enhanced green fluorescent protein (EGFP)-K5] and grown as confluent monolayer cultures. We show that keratin in these cells exists not only as intermediate filaments but also in the form of small dynamic particles. Keratin particles are found throughout the cell. Their movement is aligned with microtubules and inhibited by nocodazole, and it can be both plus-end- and minus-end-directed. A population of particulate keratin structures can also be detected in untransfected cells using scanning and transmission electron microscopy (EM) combined with immunogold labelling. The data suggest that keratin particles may be a constitutive part of keratin intermediate filament network dynamics, representing an as yet uncharacterized stage in keratin filament turnover in living cells.

Materials and Methods

Fluorescently tagged expression constructs

The full-length wild-type K5 cDNA was re-cloned from a pcDNA3 vector (clone provided by C.S. Shemanko) into pEGFP-C2 (Clontech, Basingstoke, UK) using *EcoRI* and *HindIII* restriction enzymes (EGFP-K5 clone provided by D. Gibbs). The mutant pEGFP-K5 N176S construct was made using the Quik-Change Site-Directed Mutagenesis kit (Stratagene, Amsterdam, Netherlands) and the following forward and reverse primers: pN176Sf 5'-GCAGATCAAGACCCTCAGCAATAAGTTTGCCTCC-3' and pN176Sr 5'-GGAGGCAAACCTATTGCTGAGGGTCTTGATCTG-3'. The enhanced yellow fluorescent protein (EYFP)-tubulin construct was obtained by cloning a PCR-amplified full-length cDNA sequence of α -tubulin into the *XhoI* and *BamHI* sites of the pEYFP-C1 vector (Clontech). Before use, the newly generated constructs were transfected into epithelial cells, fixed 3 days after transfection and stained to ensure that the transfected tubulin and keratin were being expressed, integrated and colocalized with the endogenous microtubule or keratin filament network (data not shown).

Cell culture and transfection

Immortalized human keratinocytes (NEB-1) (Morley et al., 1995) were cultured in Dulbecco's modified Eagle's medium (DMEM) with 25% Ham's F12 medium, 10% fetal calf serum (FCS) and growth factors hydrocortisone (0.4 μ g/ml), cholera toxin (10^{-10} M), transferrin (5 μ g/ml), lyothyronine (2×10^{-11} M), adenine (1.9×10^{-4} M) and insulin (5 μ g/ml). PtK2 cells (potoroo kidney simple epithelial cells) were cultured in a 1:1 mixture of DMEM and Ham's F12 growth medium supplemented with 10% FCS and 1% L-glutamine. Human lens cells (H36CE1) were cultured in DMEM supplemented with 10% FCS. All cell lines were grown (without feeder cells) at 37°C and 5% CO₂, either directly in plastic tissue culture grade dishes or on 13 mm or 40 mm diameter coverslips (BDH, Lutterworth, UK) for transfection experiments. Cells for transfection were cultured on

coverslips until 50% confluent, then transfected using the FuGene 6 (Boehringer Mannheim, Lewes, UK) transfection reagent (according to the manufacturer's instructions) plus 0.5–1 µg of plasmid DNA per 2 ml of serum-free medium. In double-transfection experiments, both plasmid DNAs were mixed at 1:1 ratio and incubated with the FuGene 6 reagent. Cells were incubated with the transfection reagent for 24 hours at 37°C, after which the culture medium was replaced with fresh medium and cells were further incubated for another 48 hours. By 3 days after transfection, cells grown on the coverslips were confluent and the newly expressed fluorescent proteins from the transfections were fully incorporated into the cytoskeleton.

De novo filament network assembly

The K14pcDNA3 vector (clone provided by C. S. Shemanko), encoding full-length wild-type keratin 14, was mixed in a 1:1 ratio with either the EGFP-K5 or the wild-type K5pcDNA3 construct. The mixture was then used to transfect (as above) human lens cells grown on 13 mm coverslips. Any keratin intermediate filament network formed as a result of this transfection must be formed *de novo*, as lens cells do not express keratins. Cells were fixed with methanol/acetone (1:1) at 1, 2 and 3 days post transfection. The K5/K14 pcDNA3 expression products were detected by immunofluorescence, using as primary antibody mouse monoclonal anti-K14 (LL001) (Purkis et al., 1990) with FITC-labelled sheep anti-mouse serum (Sigma) as the secondary antibody.

Live-cell imaging

Confluent coverslips of live cells were assembled in a perfusion open-closed chamber (POC chamber, H. Saur, Reutlingen, Germany). A heater was used to keep the chamber temperature constant at 37°C during imaging. Images (512×512 dpi, 2×2 binning) were collected using a 100× 1.4 NA oil immersion objective on a Nikon inverted TE200 Eclipse epifluorescence microscope equipped with a fully motorized Z stage (Applied Precision, Issaquah, USA) and linked to a Micromax CCD camera (Roper Scientific, Trenton, USA), part of the DeltaVision imaging system (Applied Precision). Stacks of optical sections spaced 200–500 nm apart were collected at each time-point (20–30 second time-lapse intervals) and subsequently deconvolved and analysed using softWorX software (Applied Precision). The softWorX 'edge enhance' tool was used for analysing images acquired in double-labelling experiments. For Figs 4 and 9, stacks of optical sections were spaced 100 nm apart. In the case of Fig. 4/Movie 5, the time lapse between time-points was shortened to 5 seconds.

Treatment of cells during live-cell imaging

Cells expressing the fluorescent constructs were selected with the 'mark and visit' tool of softWorX 2.50. Before the treatment, cells were imaged for 5 minutes with a 20 or 30 second time lapse. To depolymerize microtubules, the cell culture medium in the perfusion chamber was supplemented with nocodazole to a final concentration of 10 µg/ml. In heat-shock experiments, the temperature in the POC chamber was raised to 45°C and maintained constant for 15 minutes. The temperature was then lowered back to 37°C. In both cases (nocodazole treatment and heat shock) images were taken at fixed time-points 30 minutes, 1 hour and 2 hours after the treatment.

Immunofluorescent labelling of the cytoskeleton in untransfected PtK2 cells

PtK2 cells grown on 13 mm coverslips were fixed in a solution containing 4% paraformaldehyde, 0.1% glutaraldehyde and 0.3% Triton X-100 in cytoskeleton buffer (CB) at pH 6.1 (CB buffer contains 10 mM MES, 150 mM NaCl, 5 mM EGTA, 5 mM MgCl₂,

5 mM glucose). This fixative has previously been successfully used for EM studies (Small, 1988; Mies et al., 1998). Cells were fixed for 15 minutes and washed with CB buffer (3×10 minutes). Sodium borohydride (500 µg/ml in CB buffer, incubations on ice, 3×10 minutes), followed by washing in CB buffer, was used to quench background staining due to glutaraldehyde. Primary antibodies used were a mouse monoclonal antibody against α -tubulin (Amersham, Little Chalfont, UK) and CAM5.2 (Becton-Dickinson, Oxford, UK), a mouse monoclonal antibody recognizing K7/K8. The incubations were carried for 1 hour at room temperature, or overnight at 4°C. After extensive washing with PBS (6×10 minutes if overnight incubation), FITC-labelled sheep-anti mouse immunoglobulin was applied as secondary antibody (1 hour incubation). Coverslips were then washed again with PBS and mounted with Hydromount (National Diagnostics, Hessle, UK) supplemented with Dabco (2.5%) as antileaching reagent. Actin filaments were stained with rhodamine-labelled phalloidin (Molecular Probes, Leiden, Netherlands).

Scanning and transmission EM

The same fixative as above was used to prepare untransfected PtK2 cells for scanning and transmission EM with immunogold labelling. Cells were grown either on small squares of silicone wafer coated with L-polylysine (for scanning EM) or on CELLocate coverslips (Eppendorf) with a 175 µm square (for transmission EM). For keratin immunolocalization, cells were incubated overnight at 4°C in CAM5.2 antibody, washed in PBS (6×10 minutes), incubated for 4 hours with rabbit anti-mouse secondary antibody, washed again with PBS (5×10 minutes) and incubated overnight with a Protein A–8 nm gold conjugate. After a series of washes with PBS (4×10 minutes), cells were postfixed with 2% glutaraldehyde in PBS (30 minutes) and washed with PBS (2×15 minutes).

For scanning EM, cells were then dehydrated through graded alcohols and critical-point dried, coated with 2 nm of chromium (Cr) and viewed with a Hitachi S-4700 field emission scanning electron microscope. Images were acquired at a running voltage of 15 kV using the SE (secondary electrons) and YAGBSE (backscattered electrons) detectors.

For transmission EM, coverslips with immunostained cells were fixed for 30 minutes in 1% osmium tetroxide (OsO₄) solution, washed in PBS and dehydrated through graded alcohols, and soaked in propylene oxide (2×15 minutes) before overnight infiltration in Durcupan resin (Sigma) and propylene oxide (1:1) followed by Durcupan resin. Coverslips were then inverted onto gelatine capsules filled with resin and left to polymerize at 40°C. At this point, coverslips were snapped off the capsules, exposing the cell monolayer at the surface of the resin blocks. Sections of about 70 µm thickness were mounted onto copper grids and stained with 1% uranyl acetate and lead citrate before viewing in a JEOL 1200 EX transmission electron microscope equipped with the Fuji FDL5000 digital plate reader.

Results

Dynamic movement of keratin particles

To ascertain the ability of the transfected EGFP-K5 protein to form a functional keratin intermediate filament network, two sets of lens epithelial cells (H36CE1) were transfected in parallel with either the EGFP-K5pcDNA3 and K14pcDNA3, or K5pcDNA3 and K14pcDNA3, constructs. Lens cells do not otherwise express keratins, so any formation of a keratin filament network would have to be *de novo*. Fig. 1 shows representative images of keratin filament formation in lens cells transfected with EGFP-K5/K14pcDNA3 constructs at 1–3 days after transfection, in comparison with cells transfected

with keratin without EGFP. In both cases filaments began forming around the nucleus by day 1, and proceeded to extend into a keratin filament meshwork by days 2-3. The EGFP-K5 transfectants appeared a little slower at extending their networks than the K5 without EGFP transfectants, but the networks were indistinguishable by day 3. Thus, the EGFP-K5

protein is capable of forming an extended keratin network with K14 in the absence of any wild-type K5.

When keratinocytes (NEB-1 cells) were transfected with the EGFP-K5 construct, fluorescent keratin was produced which assembled into filaments in the endogenous filament network. Other than by their fluorescence, the filaments and the filament network were indistinguishable from those in untransfected cells. Transfected cells were filmed when they reached confluence, three days after transfection. We were able to confirm the characteristic undulatory motion of keratin filament bundles as reported by others (Windoffer and Leube, 1999). Fluorescent keratin was also detected as small, highly mobile particles, which hitherto had not been detected by immunofluorescence. We could distinguish between a smaller, highly dynamic class of keratin particles (referred to henceforth in the text as fast or F particles), and a second, larger and less mobile class of particles that appeared to be associated with the keratin filament network (referred to hereafter as slow, static or S particles). To ascertain that these particles were not an artifact of EGFP per se, cells were also transfected with EGFP alone. The expressed EGFP fluorophore produced a diffuse fluorescent staining all over the cytoplasm, but no aggregates or particulate structures were observed.

Although scattered throughout the cell, the keratin particles were small and encountered infrequently; in many cases their presence was only detectable by analysing the high-resolution movies. The behaviour of keratin F particles was therefore tracked and analysed by time-lapse filming. Fast F particles were seen to move around the cell with a saltatory type of movement, as shown in Fig. 2 (Movie 1) and Fig. 3 (Movie 2). They moved in a non-random way, following trajectories with a characteristic zig-zag appearance, and alternating between leaps and pauses during which their direction may have changed. The size of keratin particles was determined to be between 30 and 70 nm by measuring them with the 'measure distances' tool from softWorX and dividing this value by a correction factor of 6 to account for the resolution limitations of an epifluorescence microscope. The

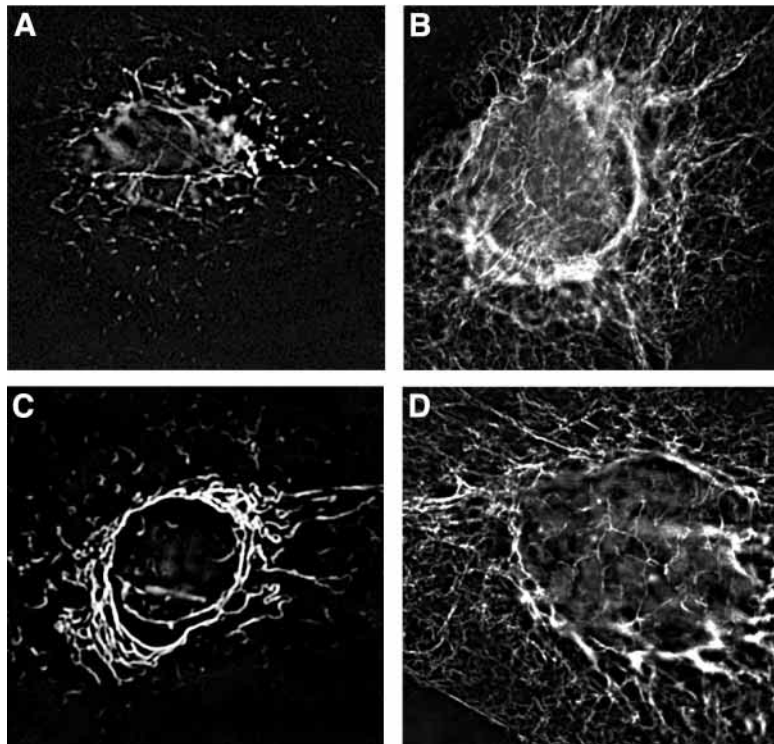


Fig. 1. De novo keratin filament polymerization. To test the capability of the EGFP-K5 fusion protein to form a functional keratin filament network, human lens cells (which otherwise do not express keratins) were transfected with either EGFP-K5/K14 pcDNA3 (A, B) or K5/K14 pcDNA3 (C, D) constructs (see Materials and Methods). At day 1 after transfection a perinuclear ring of keratin filaments is formed in both cases (A, C). At day 2, a keratin filament network is formed in lens cells transfected with the K5/K14 pcDNA3 constructs (D). Extended network formation with the EGFP-K5/K14 pcDNA3 constructs was slightly slower, but by day 3 (B), the network produced was indistinguishable from that of the K5/K14 pcDNA3-transfected cells.

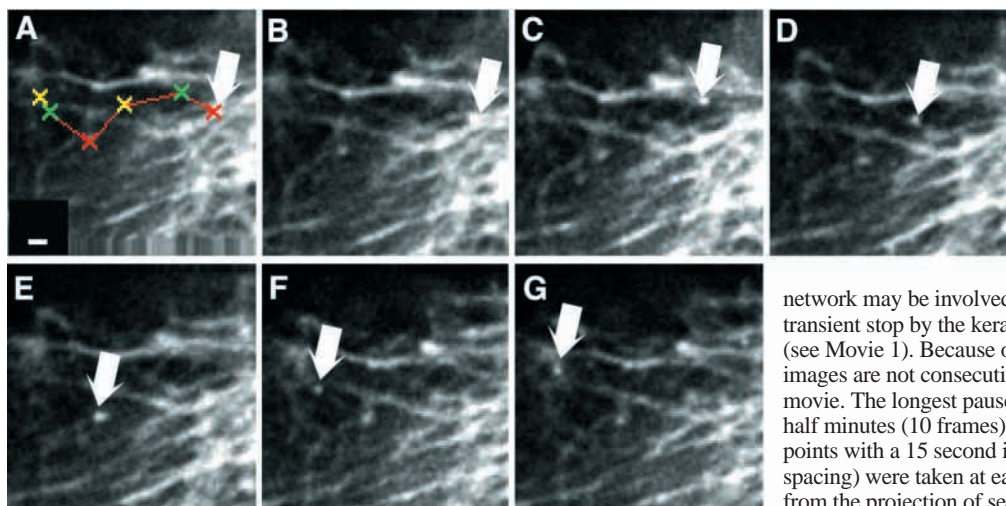


Fig. 2. Dynamic movement of a keratin F particle at the cell periphery (Movie 1). Keratinocytes (NEB-1 cells) transfected with the EGFP-K5 construct were filmed three days after transfection. (A) The course of a fast, keratin F particle. The total distance covered by the particle in 10 minutes is 11 μ m. (B-G) Reconstruction of the zig-zag movement of the keratin particle (white arrow). The keratin

network may be involved in this non-random movement, as a transient stop by the keratin particle during the saltatory movement (see Movie 1). Because of the variable lengths of the pauses, these images are not consecutive frames of the corresponding time-lapse movie. The longest pause in this sequence (C) lasted two and a half minutes (10 frames). The movie sequence contains 41 time-points with a 15 second interval, and 7 Z sections (200 nm spacing) were taken at each time-point; images were obtained from the projection of sections 5 and 6. Bar, 1 μ m.

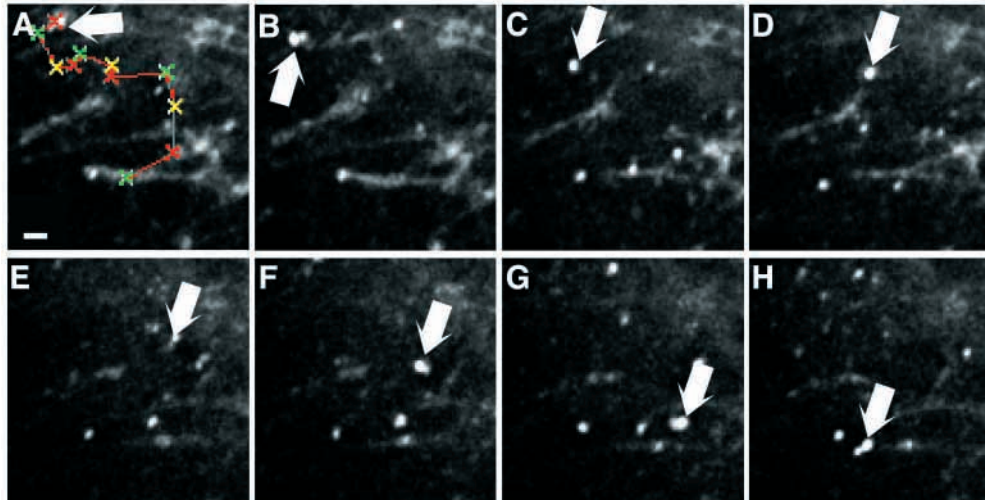


Fig. 3. Movement of a keratin F particle through the cell (Movie 2). (A) Course of a keratin F particle in a keratinocyte (NEB-1) expressing EGFP-K5, tracked over 10 minutes. (B-H) Individual time-points from this sequence; the position of the particle is indicated by the white arrow. During imaging, the particle travelled a distance of 18 μm . The courses of several other F keratin particles are seen to converge in Movie 2. Some slow, S keratin particles appearing tethered to the keratin network are visible (bottom part of B-H). The S particles moved only slightly, with an oscillatory motion around a central axis. As in Fig. 1, the keratin filament network appears to be involved in the particle movement (B-D); the longest pause (here in D, 3 minutes) occurs when the particle is located over a keratin filament. The movie covers 41 time-points with a 15 second interval, and 9 Z sections (500 nm spacing) were taken for each time-point; images were obtained by projection of sections 5 and 6. Bar, 1 μm .

correction factor was calculated by comparing the difference between the similarly determined diameter of microtubules (labelled with the EYFP-tubulin construct) and their known actual diameter of about 25 nm. The speed of individual leaps of keratin particles was calculated to be greater than 100 nm/s ($n=16$, calculated by dividing the distance travelled by the particle in a single leap by the time elapsed between the frames), suggesting the involvement of motor proteins. The length of the pauses appeared to be random, as they varied from as little as 15 seconds to over 3 minutes (see Fig. 3).

Another feature of F particle movement is the close association of the particles with keratin intermediate filament bundles during the 'pause' periods. Although the movement of the F particles does not appear to occur along keratin filaments, nevertheless the keratin network is used as a transient stop to the particles during the saltatory movement. This was particularly visible not only in Fig. 3 (Movie 2), but also, to a certain extent, in Fig. 2 (Movie 1).

By contrast, the S particles moved in a more restricted way. They appeared to be tethered, or linked, to the keratin filament network, and moved only slightly with an irregular oscillating type of motion around a fixed point (see Movie 2).

The movement of F particles is associated with microtubules

Keratinocytes (NEB-1 cells) expressing the EGFP-K5 construct were treated with the microtubule-depolymerizing drug nocodazole (10 $\mu\text{g/ml}$). Fig. 4 shows the dynamic movement of a keratin F particle before the addition of nocodazole to the cell culture medium. In the corresponding movie (Movie 3), several other F particles and a few S particles are also visible. After the drug is added to the cell culture medium (Fig. 4E-F; Movie 4), the wave-like movement of

keratin intermediate filaments slows down (compare Movies 3 (before) and 4 (after the addition of nocodazole)), and only S keratin particles remain visible. These results suggest that the saltatory motion of the F particles is dependent on intact microtubules, and the speed at which they normally move suggests the involvement of microtubule motor proteins.

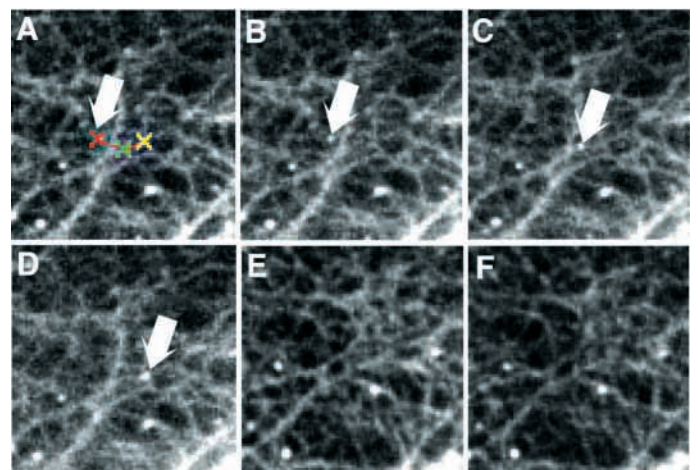


Fig. 4. Nocodazole inhibits keratin particle movement (Movies 3 and 4). Panel A traces the course of one particle among the several visible keratin F particles in Movie 3, before treatment with nocodazole. Panels B-D are consecutive (20 second interval) frames, depicting the particle's movement (arrow). Panels E and F are two frames, taken several minutes apart, of Movie 4, after the addition of nocodazole (10 $\mu\text{g/ml}$). Nocodazole stops both F keratin particle movement and keratin filament wave-like motion (compare Movies 3 and 4). Both movies were compiled from 16 images taken at 20 second intervals. Z sections were taken with a 200 nm spacing. Images in A-F were obtained by projection of sections 4 and 5.

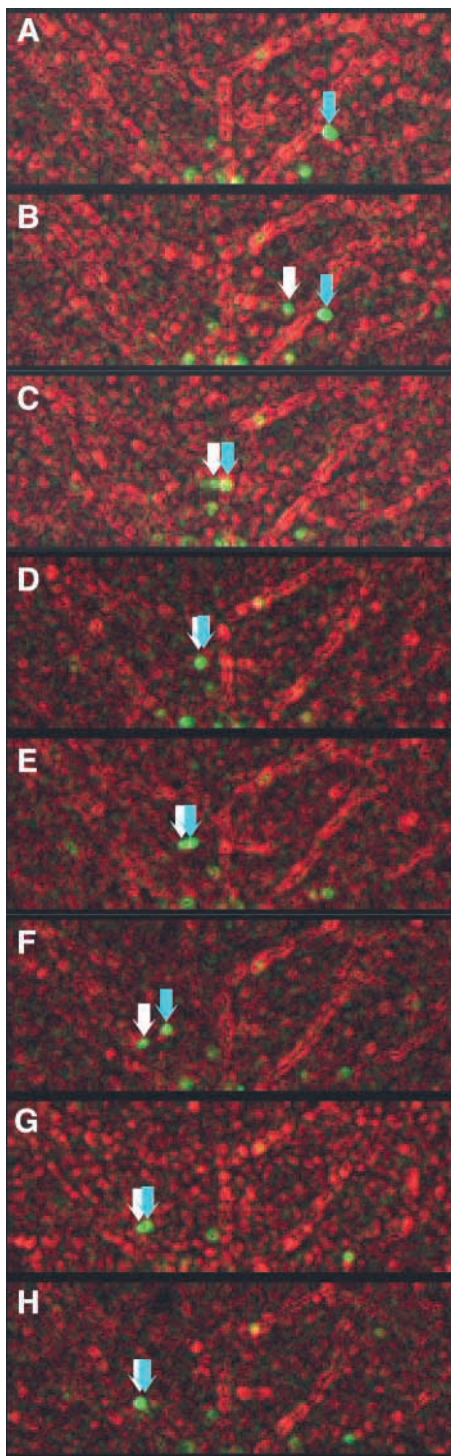


Fig. 5. Colocalization of keratin particles and microtubules (Movie 5). PtK2 cells were transfected with EGFP-K5 and EYFP-tubulin. Cells were grown to confluence, three days after transfection. Panels A-H show the path of two fast-moving F particles (white and blue arrows). In total, 34 images were acquired with a 5 second time-lapse interval (see Movie 5). Six Z sections with a 100 nm spacing were taken per time-point and subsequently analysed using the edge enhancement tool (represents filaments as tubes rather than lines) of softWorX 2.50 software. The resulting images for section 1 are shown in A-H. Two keratin particles (in green, indicated by the white and blue arrows) follow one another along the same path of a microtubule (red, positioned slightly out of the focal plane; see Movie 5).

To visualize both keratin and tubulin cytoskeletal components *in vivo* simultaneously, PtK2 cells were transfected with an EGFP-K5 keratin and an EYFP-tubulin construct. Acquired images (Fig. 5) were deconvolved and subsequently further processed using the edge enhancement algorithm of the softWorX image analysis software, which presents both keratin intermediate filaments and microtubules as tubular rather than linear structures. This significantly improved the visualization of keratin particles in images obtained from double-transfection experiments. Fig. 5 (Movie 5) shows two keratin particles (labelled green, see arrows) apparently following an identical course and briefly stopping at the same 'pause' points. Their trajectory is colocalized (yellow signal) with the course of a microtubule (in red) that is situated slightly outside the focal plane of the keratin particle. In other cases the particles also exhibited changes in the direction of their translocation through the cell, following zig-zag courses superimposed over intersecting lengths of microtubule tracks (data not shown). This reinforces the possibility that F particles are using motor proteins running on microtubule tracks to achieve fast dispersal through the cell.

Keratin particles move both towards and away from the centrosome

Imaging of keratin particles was constantly hindered by their low numbers and high speed. Previous work in this laboratory

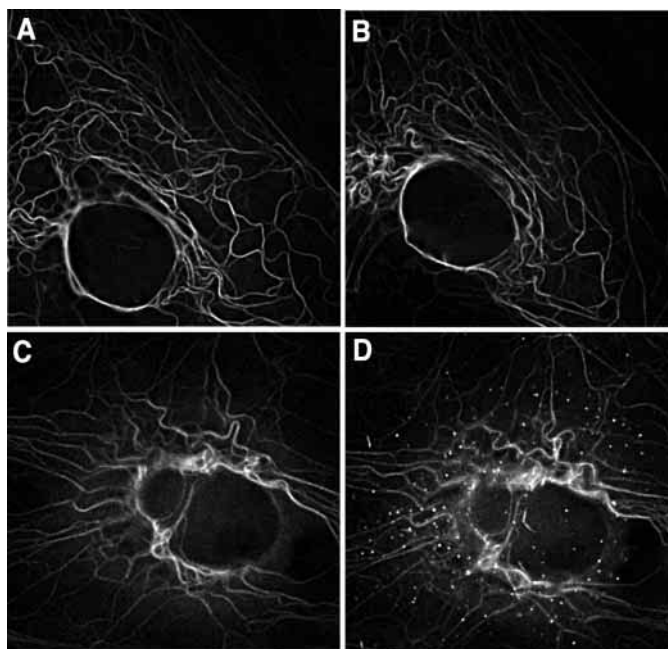


Fig. 6. Effect of heat shock on PtK2 cells transfected with wild-type (EGFP-K5) and mutant (EGFP-K5 N176S) keratin constructs. (A,B) PtK2 cell expressing EGFP-K5 before (A) and 1 hour after (B) heat shock (15 minutes at 45°C). (C,D) PtK2 cell expressing the EGFP-K5 N176S construct, again before (C) and 1 hour after (D) heat shock. The mutant keratin incorporates well into the endogenous network (C, before heat shock). After heat shock, tiny keratin particles appear in the cell expressing the mutant keratin (D), but not in the wild-type cell (B). Again, two types of particles can be distinguished: fast moving F particles and larger slow S particles that appear to be tethered to the keratin filament network (see Movie 6).

has shown that filaments incorporating pathogenic mutant keratins can be selectively destabilized by a transient shift in temperature (Morley et al., 1995). We hypothesized that this phenomenon could be used to increase the non-filamentous pool of keratin in the cell and thus possibly to amplify the number of particles, which would facilitate their observation. We selected a K5 mutation with a strong negative effect, N176S, and engineered an EGFP construct with the mutation. This K5 N176S mutation was previously identified in a patient with a severe, Dowling-Meara, form of epidermolysis bullosa simplex (Stephens et al., 1997). PtK2 cells were then transfected with either the EGFP-K5 or EGFP-K5 N176S construct. Both the wild-type (Fig. 6A) and the mutant K5 constructs (Fig. 6C) were incorporated into the endogenous keratin network. When transfected cells were subjected to heat shock, cells expressing the mutant keratin gradually developed changes in their phenotype up to a peak by 1 hour after their exposure to a thermal stress (15 minutes at 45°C), showing a significant increase in the number of visible keratin particles

(Fig. 6D; Movie 6). Here, again, the two types of keratin particles – fast-moving F particles and slower S particles – were distinguishable (see Movie 6). The S particles changed their positions only slightly, shifting with an oscillatory type of motion around a central point and during longer time intervals. Cells expressing the wild-type keratin construct remained unaffected and showed no increase in particle numbers (Fig. 6B).

To determine the directionality of the movement of the F keratin particles, we used the centrosome as a reference point for minus end anchorage of microtubules. In double-labelling experiments cells were transfected with the EGFP-K5 (or EGFP-K5 N176S) and EYFP-tubulin constructs, and keratin particle number was boosted by a 15 minute heat shock (at 45°C) before imaging.

Figs 7 and 8 show keratin particles moving along microtubule tracks. In Fig. 7, a keratin particle positioned at the periphery of the centrosome area attaches to a microtubule (Fig. 7B) and slides along it away from the centrosome (Fig.

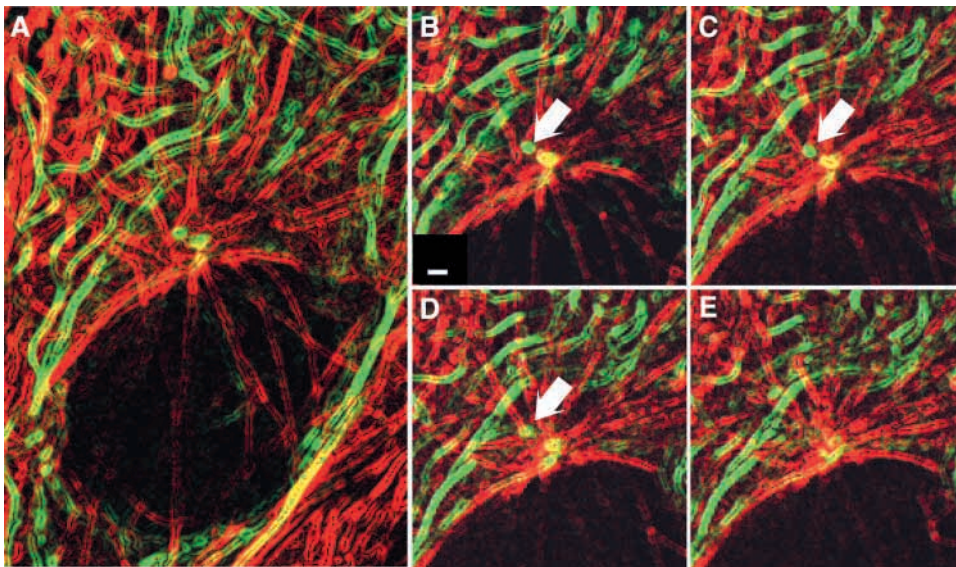


Fig. 7. A keratin particle moving away from the centrosome (Movie 7). PtK2 cells were transfected with EGFP-K5 (green) and EYFP-tubulin (red). (A) The microtubule radial array and the centrosome, in close proximity to the nucleus of a transfected cell. An F particle (arrow; B,C) positioned near to the centrosome is seen attaching to a microtubule (D) and sliding along it (E). In total, 21 images were taken with a 30 second time lapse (see Movie 7). Six Z sections were taken per time-point, with a 200 nm spacing. Panel images correspond to section 3. Images were analysed with the edge enhancement tool of softWorX 2.50. Bar, 1 μ m.

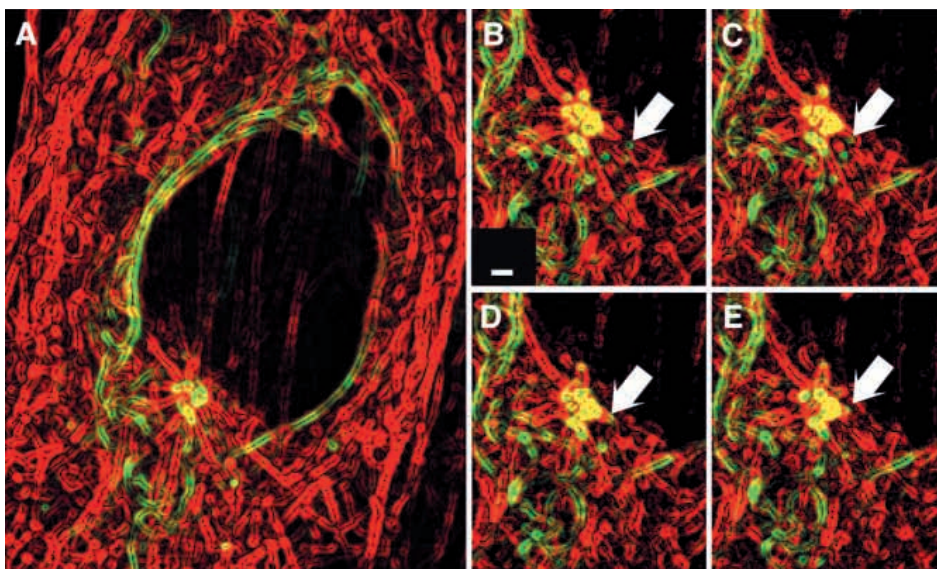


Fig. 8. A keratin particle moving towards the centrosome (Movie 8). PtK2 cells were transfected with EGFP-K5 N176S (green) and EYFP-tubulin (red). (A) The microtubule radial array and the centrosome, next to the nucleus of a transfected cell. Before imaging, cells were exposed to a heat shock to induce increased keratin particle formation. (B-E) A close-up view of the centrosome region 1 hour after the heat shock. A keratin particle (arrow) is clearly seen moving towards the centrosome and following microtubule tracks. Images from 21 time-points (see Movie 8) were collected (4 Z sections per time-point, 200 nm spacing). Panel images correspond to section 3, processed for edge enhancement. Bar, 1 μ m.

7C-D; see Movie 7). In Fig. 8, keratin particles are seen moving towards the centrosome, following microtubule tracks (see Movie 8). Thus, the movement of keratin F particles can occur in both directions (plus-end and minus-end directed), implying the involvement of more than one motor protein.

Keratin particles are also present in untransfected cells

Our results suggest that keratin particles are able to interact both with the keratin filament and the microtubule networks. We reasoned that we should also be able to detect keratin particles in fixed cells, if a fixative that allows good structural preservation of all three cytoskeletal components (keratin filaments, microtubules and microfilaments) was used. Different fixation procedures were tried, and a solution containing paraformaldehyde, glutaraldehyde and Triton X-100 (Small, 1988; Mies et al., 1998) gave by far the best results with the antibodies used. Using this fixation schedule the keratin filaments acquired a grainy or particulate quality (see Fig. 9A,B).

As this fixation procedure has been previously used for transmission EM (Small, 1988), we examined these keratin filaments by electron microscopy of untransfected PtK2 cells that had been immunogold-labelled for K8 before resin embedding. As the fixative contains a small amount of anionic detergent (Triton-X 100) to permeabilize the cells, we used this procedure to fix and label keratin filaments for scanning EM.

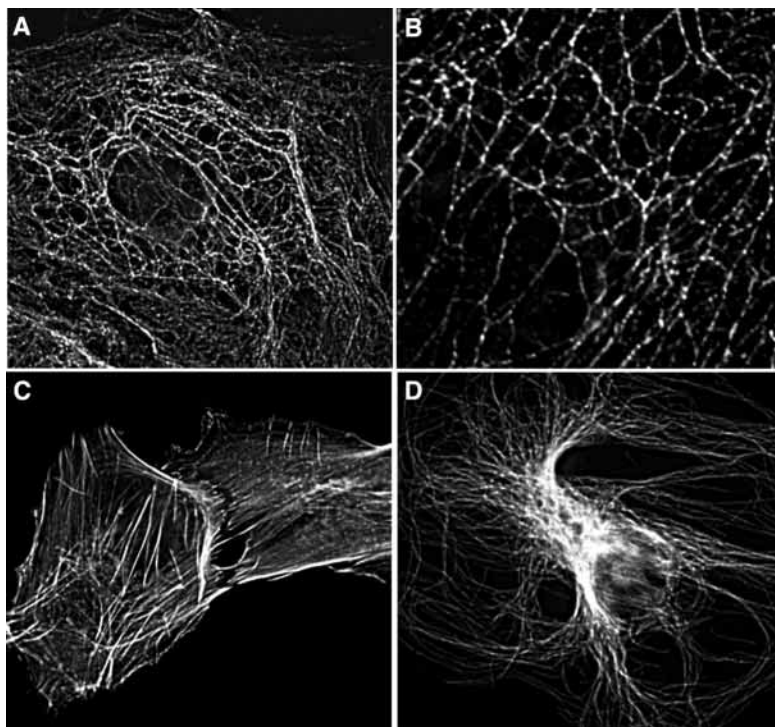


Fig. 9. Immunofluorescence of the cytoskeleton in untransfected PtK2 cells. Untransfected PtK2 epithelial cells were fixed and stained for actin, tubulin and intermediate filaments as described in Materials and Methods. Representative images are shown of the keratin filament network (K8/K18) (A,B), actin (C) and microtubules (D). Image (A) is acquired with 2×2 binning, whereas (B) is a high-resolution image (1×1 binning) showing keratin filaments in more detail. At higher power, the keratin filaments (only) have a granular appearance, which was not detected with other fixations regimes.

The cytoskeleton could then be visualized through the resulting holes in the membrane. The results are shown in Fig. 10. Both scanning and transmission EM show small localized thickenings, as well as clear particles attached to the keratin filaments, both of which clearly contain keratin. The particles are globular in shape and have a size range of about 30-60 nm, consistent with the F particles seen in living cells.

Discussion

We have obtained evidence that non-filamentous keratin protein is rapidly translocated throughout epithelial cell cytoplasm in the form of small, fast keratin particles (F particles). We have recorded these particles using GFP-tagged keratin K5, in both keratinocytes (which naturally express K5 with K14) and in simple epithelial cells (in which the K5 is supernumerary). Similar keratin particles of the same order of magnitude in size can also be detected in cells that have not been transfected with EGFP-K5, suggesting that these structures are a natural feature of keratin biology in epithelial cells and not only an artifact of overexpression of keratin or of defective behaviour of EGFP fusion proteins.

These small particles have not been described previously. In both previous reports dealing with keratin intermediate filament dynamics, spreading subconfluent cells were used. Yoon et al. (Yoon et al., 2001) compared keratin K8/K18 and vimentin intermediate filaments. Although the authors used PtK2 cells (as we did), fast keratin particles were not reported. Instead, larger short filament fragments located at the cell periphery (squiggles) were seen – structures that had also been identified previously in vimentin networks (Yoon et al., 1998). Windoffer et al. (Windoffer et al., 1999) looked at A431 cells and, by tracking EGFP-K13, they observed structures formed by the constant fusing, extending and branching of keratin filaments during their inwardly oriented wave-like translocation. Fast-moving keratin particles were not reported in this study either, although after careful examination we could see several of them in one of their published time-lapse films (Windoffer and Leube, 1999) (Movie 3, ‘without nocodazole’). The fact that the A431 cells used in that study were stably transfected with EGFP-K13 also illustrates that the keratin particles are not a short-term artifact of transfection.

Working with confluent cell cultures enabled us to observe two distinct types of keratin particles: F particles, which are very dynamic and have a saltatory pattern of movement, and S particles, which appear to be tethered to the keratin filaments and have only a limited, oscillatory motion. The movement of the F particles consists of alternating fast ‘leaps’ with interspersed ‘pauses’ of variable length, resulting in a characteristic zig-zag trajectory through the cytoplasm. This motion bears a striking similarity to fast axonal transport, the translocation of neurofilaments along axons (Wang et al., 2000b). Transport of the F particles occurs at high speed and is aligned with microtubules. Fast-moving particles in interphase cells have been described for vimentin

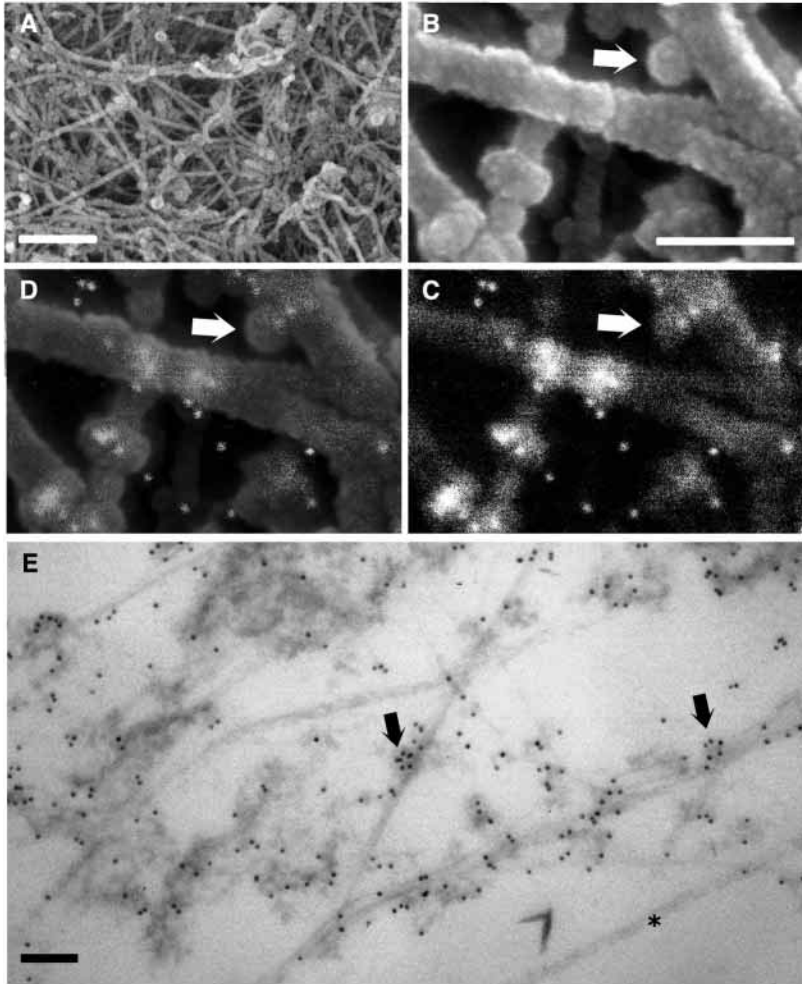


Fig. 10. Field emission scanning and transmission EM of untransfected PtK2 cells. Untransfected PtK2 cells were fixed and immunogold labelled (with 8 nm gold particles) for K8, a natural component of the endogenous keratin filament network, as described in Materials and Methods. (A) Scanning EM image to show the degree of cytoskeleton preservation; image acquired using the SE detector (secondary electrons), at 9000 \times magnification and 10 mm working distance. Bar, 1 μ m. (B,C,D) The keratin filament cytoskeleton at high magnification. All images were taken at 130,000 \times magnification and a working distance of 10.1 mm. Image in (B) was acquired using the SE detector to show maximum detail of the keratin filament surface structure. Image in (C) was acquired with the YAGBSE detector for backscattered electrons, to distinguish gold particles of the immunogold labelling; gold particles appear as white dots on the filaments from the high-energy backscattered electrons, but the image of the filament surface is poor. Both SE and YAGBSE images are combined in (D), where a keratin particle attached to the side of a keratin filament can be clearly seen (white arrow). Bar, 100 nm. (E) Transmission EM image of cell after the same fixation as in (A-D), also labelled with anti-K8 monoclonal antibody CAM 5.2. Immunogold labelling was performed before resin embedding and labelling is seen (black dots) along the keratin filaments. Keratin particles are seen adhering to the filaments (black arrows). Note that microtubules (*) are unlabelled. Bar, 100 nm.

intermediate filaments (Prahlad et al., 1998) and for neurofilaments (Prahlad et al., 2000). Prahlad et al. (Prahlad et al., 1998) looked at vimentin particles in spreading BHK-21 cells: the particles were most pronounced at the cell periphery, where they were seen to fuse into vimentin 'squiggles' and short fibrils. In our experiments, 'squiggles' were not observed. As we were looking at the cytoskeleton in cultured cells grown as confluent monolayers, cell translocation was minimal. It is possible that the intermediate filament (keratin and vimentin) structures referred to as 'squiggles' are specifically associated with bulk transport or rearrangements of the intermediate filament protein network around the cell edge in spreading or mobile cells.

Both our findings (for keratin) and those for vimentin and neurofilaments (cited above) show that fast transport of intermediate filament particles depends on, and is associated with, microtubules. The vimentin particles were seen in early stages of spreading and were suggested to interact with the microtubule plus-end-directed motor protein kinesin (Prahlad et al., 1998). Most recently, Helfand et al. (Helfand et al., 2002) have suggested that some structural forms of vimentin can also be associated with subunits of dynein and dynactin, implying that bidirectional transport of vimentin is possible. Our results on keratin intermediate filaments concur with those on

vimentin, as we have shown that the keratin F particles are able to move both towards (minus-end directed) and away from (plus-end directed) the microtubule organizing centre of the centrosome. Neurofilament particles have been shown to be associated with at least one type of kinesin motor protein *in vivo* (Prahlad et al., 2000), but bidirectionality in their movement is yet to be shown.

Keratin filaments may have an active role in this bidirectional transport of keratin particles. In our time-lapse films, filaments appear to function as anchor points during the 'pause' phase, a detail previously unreported for other intermediate filament fragments and particles. The zig-zag trajectory also seems to be an intrinsic characteristic of the keratin F particles. One possible model accounting for the observed movement would be that keratin particles 'hitchhike' on microtubule motors to traverse micrometre-long distances in a matter of seconds, and the keratin filaments are used as temporary 'anchoring' points while waiting for motor protein(s) to pass close enough for the F particles to adhere to them. The dense microtubule network would also enable the keratin particles to switch between different microtubule tracks, thus giving rise to the zig-zag travel pattern. Such movement between two cytoskeleton systems would obviously be dependent on maintaining structural links between the

systems, as effected by 'cytolinker' proteins such as plectin (Svitkina et al., 1996; Svitkina et al., 1998) and possibly other plakins.

What are these keratin particles and why were they not detected before? Keratin aggregates have often been observed during large-scale intermediate filament network rearrangements in cells. As well as the diagnostic keratin aggregates of EBS, keratin aggregate formation was reported in cells undergoing mitosis (Lane et al., 1982), during the assembly and disassembly of the keratin intermediate network in live dividing cells (Windoffer and Leube, 2001), and during keratin filament breakdown in epithelial cells induced by the treatment with okadaic acid (Strnad et al., 2001) or keratin antibody microinjection (Klymkowsky et al., 1983). Many of these rearrangements require phosphorylation, which destabilizes filaments and drives the equilibrium towards depolymerization, leading to aggregate formation (Inagaki et al., 1996; Omary et al., 1998; Feng et al., 1999; Sahlgren et al., 2001). The use of phosphatase inhibitors on live cells – pervanadate (Windoffer and Leube, 2001) and okadaic acid by (Strnad et al., 2001) – has confirmed a correlation between increased keratin phosphorylation levels, and filament breakdown and aggregate formation. Although these previously described keratin aggregates are all much larger structures than the keratin particles we describe here, the aggregates may derive from condensations of smaller particles over time. There are also several technical reasons that can help to explain why they have been overlooked until now. For example, a single still image cannot identify an object that is characterized only by its movement. Additionally, methanol and acetone, the inorganic solvents most often used to fix cells for intermediate filament visualization, are weak fixatives that do not preserve more delicate structures – such as membranes, microfilaments, microtubules and possibly other structures interacting with them – to the same extent. Therefore, small and soluble structures may simply be washed out during processing.

Most of the data on stages of intermediate filament assembly have been derived from in vitro polymerization studies, and their counterparts in live cells still need to be identified. Considering the keratin particle size, the bidirectionality of their dispersal system, the fact that the visible keratin particle pool was significantly increased in stressed cells expressing mutant keratin and that particles were found in nontransfected cells as well, it is highly possible that keratin particles may be a constitutive part of the regulation and maintenance of the keratin intermediate filament network in cells. We are currently limited by available technology in defining their origin and function, but one look at the three-dimensional density of cytoskeleton filaments in the cytoplasm of these cells (Fig. 10A), and the frequency of intersections between them, emphasizes the potential of a system that could disperse small keratin particles rapidly along and across such structures. The small fast keratin particles may be oligomeric assemblies of keratin, which may represent the live-cell counterpart of the 'unit length filaments' found in vitro. However, they may also represent hyperphosphorylated oligomers, which are transiently in an unfavourable configuration for incorporation into filaments (Omary et al., 1998), and while some may be destined for degradation (Toivola et al., 2002), others may eventually get incorporated into filaments. Although the size

of the particles currently makes it difficult to identify them conclusively by other means than live-cell imaging, this study does emphasize the need for detailed analysis of keratin dynamics so that new routes to intervention therapy for EBS and related skin fragility diseases can be identified.

Very special thanks for their advice, support and the best of company during the long hours of EM work to John James, Calum Thomson, Martin Kierans and Euan James at the Center for High resolution Imaging and Processing in Cell and Molecular Biology (CHIPs, www.dundee.ac.uk/biocentre/chips), School of Life Sciences, University of Dundee. We also thank Paul Andrews and Jason Swedlow in our institute for their assistance with the use of the DeltaVision imaging system, and Pat Ogden and Mariella D'Alessandro for their help with cell culture. We also thank C. S. Shemanko and D. Gibbs for the pcDNA3K5 and PEGFP-K5 constructs, which they generated while in this lab. This work was supported by the Wellcome Trust (055090/A/98/Z, to E.B.L.) and the Ministry of Science and Technology of the Republic of Slovenia (Z3-3310-0381-01, to M.L.).

References

- Anton-Lamprecht, I. and Schnyder, U. W.** (1982). Epidermolysis bullosa herpetiformis Dowling-Meara. Report of a case and pathomorphogenesis. *Dermatologica* **164**, 221-235.
- Chou, C. F., Riopel, C. L., Rott, L. S. and Omary, M. B.** (1993). A significant soluble keratin fraction in 'simple' epithelial cells. Lack of an apparent phosphorylation and glycosylation role in keratin solubility. *J. Cell Sci.* **105**, 433-444.
- Coulombe, P. A. and Omary, M. B.** (2002). 'Hard' and 'soft' principles defining the structure, function and regulation of keratin intermediate filaments. *Curr. Opin. Cell Biol.* **14**, 110-122.
- Feng, L., Zhou, X., Liao, J. and Omary, M. B.** (1999). Pervanadate-mediated tyrosine phosphorylation of keratins 8 and 19 via a p38 mitogen-activated protein kinase-dependent pathway. *J. Cell Sci.* **112**, 2081-2090.
- Haneke, E. and Anton-Lamprecht, I.** (1982). Ultrastructure of blister formation in epidermolysis bullosa hereditaria: V. Epidermolysis bullosa simplex localisata type Weber-Cockayne. *J. Invest. Dermatol.* **78**, 219-223.
- Helfand, B. T., Mikami, A., Vallee, R. B. and Goldman, R. D.** (2002). A requirement for cytoplasmic dynein and dynactin in intermediate filament network assembly and organization. *J. Cell Biol.* **157**, 795-806.
- Herrmann, H. and Aebi, U.** (1998). Intermediate filament assembly: fibrillogenesis is driven by decisive dimer-dimer interactions. *Curr. Opin. Struct. Biol.* **8**, 177-185.
- Herrmann, H., Haner, M., Brettel, M., Ku, N. O. and Aebi, U.** (1999). Characterization of distinct early assembly units of different intermediate filament proteins. *J. Mol. Biol.* **286**, 1403-1420.
- Herrmann, H., Strelkov, S. V., Feja, B., Rogers, K. R., Brettel, M., Lustig, A., Haner, M., Parry, D. A., Steinert, P. M., Burkhard, P. et al.** (2000). The intermediate filament protein consensus motif of helix 2B: its atomic structure and contribution to assembly. *J. Mol. Biol.* **298**, 817-832.
- Ho, C. L., Martys, J. L., Mikhailov, A., Gundersen, G. G. and Liem, R. K.** (1998). Novel features of intermediate filament dynamics revealed by green fluorescent protein chimeras. *J. Cell Sci.* **111**, 1767-1778.
- Inagaki, N., Tsujimura, K., Tanaka, J., Sekimata, M., Kamei, Y. and Inagaki, M.** (1996). Visualization of protein kinase activities in single cells by antibodies against phosphorylated vimentin and GFAP. *Neurochem. Res.* **21**, 795-800.
- Irvine, A. D. and McLean, W. H.** (1999). Human keratin diseases: the increasing spectrum of disease and subtlety of the phenotype-genotype correlation. *Br. J. Dermatol.* **140**, 815-828.
- Ishida-Yamamoto, A., McGrath, J. A., Chapman, S. J., Leigh, I. M., Lane, E. B. and Eady, R. A.** (1991). Epidermolysis bullosa simplex (Dowling-Meara type) is a genetic disease characterized by an abnormal keratin-filament network involving keratins K5 and K14. *J. Invest. Dermatol.* **97**, 959-968.
- Klymkowsky, M. W., Miller, R. H. and Lane, E. B.** (1983). Morphology, behavior, and interaction of cultured epithelial cells after the antibody-induced disruption of keratin filament organization. *J. Cell Biol.* **96**, 494-509.

- Lane, E. B. (1994). Keratin diseases. *Curr. Opin. Genet. Dev.* **4**, 412-418.
- Lane, E. B., Goodman, S. L. and Trejdosiewicz, L. K. (1982). Disruption of the keratin filament network during epithelial cell division. *EMBO J.* **1**, 1365-1372.
- Liovic, M., Stojan, J., Bowden, P. E., Gibbs, D., Vahlquist, A., Lane, E. B. and Komel, R. (2001). A novel keratin 5 mutation (K5V186L) in a family with EBS-K: a conservative substitution can lead to development of different disease phenotypes. *J. Invest. Dermatol.* **116**, 964-969.
- Mehrani, T., Wu, K. C., Morasso, M. I., Bryan, J. T., Marekov, L. N., Parry, D. A. and Steinert, P. M. (2001). Residues in the 1A rod domain segment and the linker L2 are required for stabilizing the A11 molecular alignment mode in keratin intermediate filaments. *J. Biol. Chem.* **276**, 2088-2097.
- Mies, B., Rottner, K. and Small, J. V. (1998). Multiple immunofluorescence microscopy of the cytoskeleton. In *Cell Biology: A Laboratory Handbook 2* (ed. J. E. Celis), pp. 469-476. San Diego, CA: Academic Press.
- Morley, S. M., Dundas, S. R., James, J. L., Gupta, T., Brown, R. A., Sexton, C. J., Navsaria, H. A., Leigh, I. M. and Lane, E. B. (1995). Temperature sensitivity of the keratin cytoskeleton and delayed spreading of keratinocyte lines derived from EBS patients. *J. Cell Sci.* **108**, 3463-3471.
- Omary, M. B., Ku, N. O., Liao, J. and Price, D. (1998). Keratin modifications and solubility properties in epithelial cells and in vitro. *Subcell. Biochem.* **31**, 105-140.
- Prahlad, V., Yoon, M., Moir, R. D., Vale, R. D. and Goldman, R. D. (1998). Rapid movements of vimentin on microtubule tracks: kinesin-dependent assembly of intermediate filament networks. *J. Cell Biol.* **143**, 159-170.
- Prahlad, V., Helfand, B. T., Langford, G. M., Vale, R. D. and Goldman, R. D. (2000). Fast transport of neurofilament protein along microtubules in squid axoplasm. *J. Cell Sci.* **113**, 3939-3946.
- Purkis, P. E., Steel, J. B., Mackenzie, I. C., Nathrath, W. B., Leigh, I. M. and Lane, E. B. (1990). Antibody markers of basal cells in complex epithelia. *J. Cell Sci.* **97**, 39-50.
- Quinlan, R. A., Cohlberg, J. A., Schiller, D. L., Hatzfeld, M. and Franke, W. W. (1984). Heterotypic tetramer (A2D2) complexes of non-epidermal keratins isolated from cytoskeletons of rat hepatocytes and hepatoma cells. *J. Mol. Biol.* **178**, 365-388.
- Sahlgren, C. M., Mikhailov, A., Hellman, J., Chou, Y. H., Lendahl, U., Goldman, R. D. and Eriksson, J. E. (2001). Mitotic reorganization of the intermediate filament protein nestin involves phosphorylation by cdc2 kinase. *J. Biol. Chem.* **276**, 16456-16463.
- Small, J. V. (1988). The actin cytoskeleton. *Electron. Microsc. Rev.* **1**, 155-174.
- Soellner, P., Quinlan, R. A. and Franke, W. W. (1985). Identification of a distinct soluble subunit of an intermediate filament protein: tetrameric vimentin from living cells. *Proc. Natl. Acad. Sci. USA* **82**, 7929-7933.
- Steinert, P. M., Marekov, L. N. and Parry, D. A. (1993a). Conservation of the structure of keratin intermediate filaments: molecular mechanism by which different keratin molecules integrate into preexisting keratin intermediate filaments during differentiation. *Biochemistry* **32**, 10046-10056.
- Steinert, P. M., Marekov, L. N., Fraser, R. D. and Parry, D. A. (1993b). Keratin intermediate filament structure. Crosslinking studies yield quantitative information on molecular dimensions and mechanism of assembly. *J. Mol. Biol.* **230**, 436-452.
- Stephens, K., Ehrlich, P., Weaver, M., Le, R., Spencer, A. and Sybert, V. P. (1997). Primers for exon-specific amplification of the KRT5 gene: identification of novel and recurrent mutations in epidermolysis bullosa simplex patients. *J. Invest. Dermatol.* **108**, 349-353.
- Strnad, P., Windoffer, R. and Leube, R. E. (2001). In vivo detection of cytokeratin filament network breakdown in cells treated with the phosphatase inhibitor okadaic acid. *Cell Tissue Res.* **306**, 277-293.
- Svitkina, T. M., Verkhovskiy, A. B. and Borisy, G. G. (1996). Plectin sidearms mediate interaction of intermediate filaments with microtubules and other components of the cytoskeleton. *J. Cell Biol.* **135**, 991-1007.
- Svitkina, T. M., Verkhovskiy, A. B. and Borisy, G. B. (1998). Plectin sidearms mediate interactions of intermediate filaments with microtubules and other components of the cytoskeleton. *Biol. Bull.* **194**, 409-410.
- Toivola, D. M., Zhou, Q., English, L. S. and Omary, M. B. (2002). Type II keratins are phosphorylated on a unique motif during stress and mitosis in tissues and cultured cells. *Mol. Biol. Cell* **13**, 1857-1870.
- Wang, H., Parry, D. A., Jones, L. N., Idler, W. W., Marekov, L. N. and Steinert, P. M. (2000a). In vitro assembly and structure of trichocyte keratin intermediate filaments: a novel role for stabilization by disulfide bonding. *J. Cell Biol.* **151**, 1459-1468.
- Wang, L., Ho, C. L., Sun, D., Liem, R. K. and Brown, A. (2000b). Rapid movement of axonal neurofilaments interrupted by prolonged pauses. *Nat. Cell Biol.* **2**, 137-141.
- Windoffer, R. and Leube, R. E. (1999). Detection of cytokeratin dynamics by time-lapse fluorescence microscopy in living cells. *J. Cell Sci.* **112**, 4521-4534.
- Windoffer, R. and Leube, R. E. (2001). De novo formation of cytokeratin filament networks originates from the cell cortex in A-431 cells. *Cell Motil. Cytoskeleton* **50**, 33-44.
- Wu, K. C., Bryan, J. T., Morasso, M. I., Jang, S. I., Lee, J. H., Yang, J. M., Marekov, L. N., Parry, D. A. and Steinert, P. M. (2000). Coiled-coil trigger motifs in the 1B and 2B rod domain segments are required for the stability of keratin intermediate filaments. *Mol. Biol. Cell* **11**, 3539-3558.
- Yoon, M., Moir, R. D., Prahlad, V. and Goldman, R. D. (1998). Motile properties of vimentin intermediate filament networks in living cells. *J. Cell Biol.* **143**, 147-157.
- Yoon, K. H., Yoon, M., Moir, R. D., Khuon, S., Flitney, F. W. and Goldman, R. D. (2001). Insights into the dynamic properties of keratin intermediate filaments in living epithelial cells. *J. Cell Biol.* **153**, 503-516.